# A new frequency analysis for diagnosis of bearing defects in induction motors using the adaptive lifting scheme of wavelet transforms

**Wafa Bentrah [1]✉, Salim Sbaa[2], Nadjiba Terki[1], Noureddine Bessous[3]**

1 *Electrical Engineering Department, Université de Biskra, B.P. 145 R.P. 07000, Biskra, Algeria*

2 *Electronic Engineering Department, Université de Biskra, B.P. 145 R.P. 07000, Biskra, Algeria*

3 *Electrical Engineering Department, Université de El-Oued, 39000 El-Oued, Algeria*

Received 29 November 2017

Published online: 10 June 2018

*Keywords*

Lifting schemes

Faults

Motor current signature analysis

Fast Fourier transforms

Diagnostic

Fault diagnosis

**Abstract:** This work describes a novel and effective application of the adaptive wavelet transform for the detection of bearing faults on induction motor stator current. This transform is based on a three-step nonlinear lifting scheme: a fixed prediction followed by a space-varying update and a no additive prediction. This transformation technique is used in a diversity of applications in digital signal processing and the transmission or storage of sampled data (notably the compression of the sound, or physical measurements of accuracy). Many faults in induction motor have been identified as bearing defects, rotor defects and external defects. Experimental results confirm the utility and the effectiveness of the proposed method for outer raceway fault diagnosis under no load and full load conditions.



## 1. Introduction

In general, when we talk about fault diagnosis, we refer to the procedure of detection. The role of this procedure is to provide information on the appearance of a defect and its provenance as quickly as possible. Since the early 1970s, the detection and localization methods of defects have considerably increased. Indeed, many researchers have invested in this domain offering various approaches and techniques for responding to the diversity of applications (Wang et al. 2018, Saidi. 2017).

The induction motor is the most used in the domain of higher powers and it has many advantages: robustness, simple construction, low cost, etc. Several faults in induction motor have been identified as bearings faults, rotor faults and external faults… (Mabrouk et al. 2017, Lebaroud and Guy 2011**)**, it can be: mechanical, electrical or magnetic. These failures can cause big losses at the level of the production for this reason it is imperative to find a diagnostic system for safe operation.

Over the last twenty years, there have been continued efforts to study and diagnosis of different defects in asynchronous machines; in particular, much work has been devoted to the problem of rotor bars faults, eccentricity static or dynamic and stator faults in addition to the development of diagnostic techniques (Yang et al. 2014, Bouzida et al. 2017, Gyftakis and Kappatou 2013). Some research work has been based on analysis of the stator current signature using the FFT technique (Bessous et al. 2015, Blödt et al. 2004) to detect electrical and mechanical faults affecting induction motors.

to provide innovative solutions to the defects of the asynchronous machine, meny work has been done in this area based on the discrete wavelet transform (DWT) this analysis consists of giving a representation of the signals allowing the simultaneous development of the temporal and frequency information (time-frequency localization) which have been used to detect the faults (Karvelis et al. 2015, Barman et al. 2015, Yahia et al. 2014).

The discovery of the lifting structure technique has a multi-resolution wavelet transforms, with a simple construction, always invertible and authorizing the implementation of nonlinear operators able to capture the singularities of a signal. The adaptive lifting scheme is a modified version of the classical one; the adaptation consists in choosing between different filters, according to local information signal, there are two adaptive lifting forms: either we begin by predicting then updating or by applying the update operator after the prediction one (Piella and Pesquet-Popescu 2005). In this context, the researchers Piella and Pesquet-Popescu (2005, 2007), Heijmans et al. (2005) and Heijmans et al. (2006) have identified a new class of adaptive wavelets.The objective of lifting scheme is to provide a simple wavelet process, reversible and fast transformation.

The objective of this study is to make a comparison between the two methods the first is known as motor current signature analysis MCSA using the FFT and the adaptive lifting scheme to confirm the effectiveness of the last one (the three -step nonlinear lifting). This paper is organized as follows. In Section2,

✉ Corresponding author. E-mail address: wafaelect@gmail.com

we talk about the diagnosis of the asynchronous machine and the criteria for selecting the defects. Section 3 discusses about the use of the three-step nonlinear lifting scheme and their application .In the fourth section, we present in detail the experimental testing. Finally, Section 5 gives the conclusion of this work.

## 2. Diagnosis of the asynchronous machine

Indeed, the asynchronous motor is one of the most appreciated in the industrial applications of small and strong powers which range from tens of thousands of kilowatts. Simply because this actuator has a lot of advantages, namely its mass, power, robustness, ease of implementation and low cost. The word diagnosis can have several interpretations depending on the context and the domain d 'application. The aims of the diagnosis of industrial processes are to find the cause of a failure or defect. The causes of the defects are multiple they can be classified into three groups: (Bonnett and Soukup 1992).

- Fault generators or initiators: motor overheating, fault electrical (short circuit), mechanical problems, rupture of fixation, insulation problem, power surge...
- Fault amplifiers: frequent surcharge, mechanical vibrations, humid environment, disturbed power supply (instability of voltage or frequency), permanent heating, bad greasing, aging etc.
- Manufacturing defects and human errors: manufacturing defects, defective components, unsuitable protections, incorrect sizing of the machine etc.

The most preoccupations of these defects are:

- The stator faults.
- Bearing defects.
- Partial or total breaks of the bars and portions of short-circuit rings of the rotor cage.
- Eccentricity defects.

Faults that occur on asynchronous machines lead to multiple problems which affect the profitability of the overall installation, and which may go as far as total shutdown.

One of the consequences of defects is:

- Fluctuations torque and speed of the induction motor.
- Additional call of current.
- Imbalance in voltage and line current.
- Increases in not programmed stops, production losses, and therefore global performance.

The analysis of a signal, therefore, is a source of information.

Indeed, the measure of a signal indicates oscillations that may be harmonic, of a stochastic nature, or two simultaneously. The variation of these signals can be related to the defects (Oumaamar et al. 2005) .To extracts the characteristics of a signal relating to a fault generally, amplitude or amplitude densities are extracted. However, there are other possibilities of determining the autocorrelation functions, the transformations of Fourier or spectral density.

### 2.1. The selection of defects

The criteria for selecting the defects studied are based on the following causes:

- Percentage and important statistics of occurrence;
- Electromagnetic phenomenon directly or indirectly affected;
- The impact on the efficiency and power of the machine;
- Consequences of the defect in the machine, the equipment, the environment and the human being;
- Objective of our application;
- Model debugging in the presence of the defect.

According to these criteria, we will retain the following defects:

- Breaking bars defects;
- Static, dynamic and mixed eccentricity defects;
- Bearing defects (outer race, inner race) ;

## 3. Three-Step Nonlinear Lifting Scheme Technique

The lifting schemes (Piella and Pesquet-Popescu 2007) include three steps shown in Figure 1:

- Transform polyphase
- Prediction Operation P
- Update Operation U

The adaptive lifting scheme is a modified version of the classic lifting, the adaptation consists in choosing between several filters, according to the local information of the signal and there are two adaptive lifting structures: either we start with the prediction then the update, either one proceeds with the application of the operator of the update then the prediction to see figure 2.

The initial idea would be to write:

$$h = x_0 - P_{adap}(x_e) \quad (1)$$

$$l = x_e + U(h) \quad (2)$$

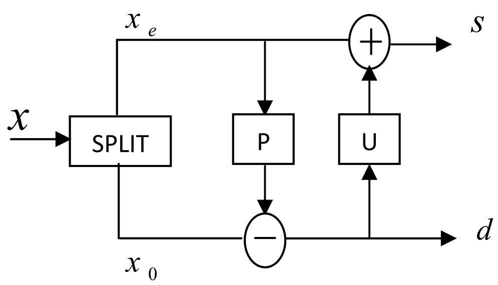


**Fig. 1.** Principle of lifting scheme.

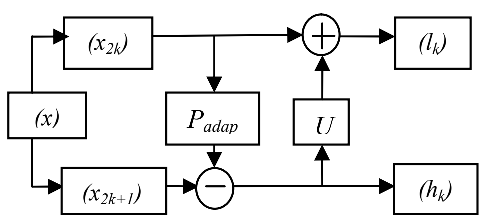


**Fig. 2.** Principle of lifting scheme, with non-linear prediction step before the update step.

Where

$$P_{adap}(x_e)(n) = \sum x_e(k) F_n(n-k) \quad (3)$$

The order of $F_n$ depends on the regularity of $x_e$ en *n*. The update structure before the prediction figure 3 is better adapted to avoid problems of stability and synchronization.

**3.1. A three-step nonlinear**

From the lifting scheme presented in Figure 4:

WT is the lazy wavelet transform**.**

H, G are thresholding operators defined for all u ∈ IR as:

$$x(n) = x_0(2n), \quad y(n) = x_0(2n-1) \quad (4)$$

$$H(u) = \begin{cases} 1/2\ u & \text{if } |u| \langle T \\ \alpha T / 2 sign(u) & \text{otherwise} \end{cases} \quad (5)$$

$$G(u) = \begin{cases} u & \text{if } |u| \succ T' \\ \alpha' T' & \text{otherwise} \end{cases} \quad (6)$$

Where $T, T'$ are positive threshold values and $\alpha, \alpha' \in \{0,1\}$ constants which determine the kind of thresholding.

The approximation signal $x'$ is deduced from the following relation:

$$x'(n) = x(n) + H(d(n) \quad (7)$$

Where *d(n)* is a first detail signal equal at *y(n)-x(n).*

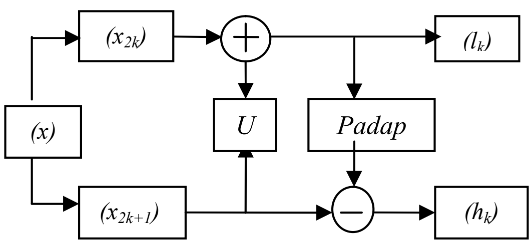


**Fig. 3.**principle of lifting scheme, with update step first, then with a non-linear prediction step.

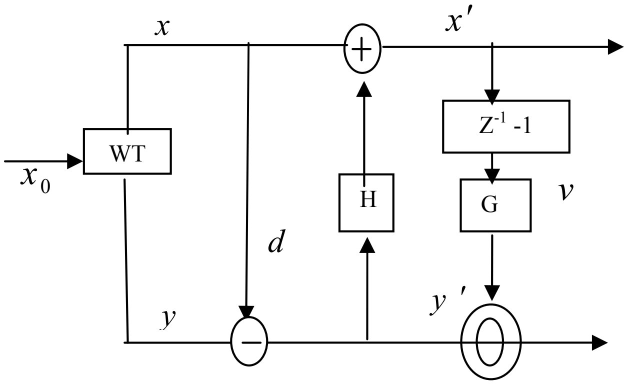


**Fig. 4.** Three-stage lifting scheme

$$\bar{y}(n) = \frac{d(n)}{B + |G(v(n))|} \quad (8)$$

Where

$$v(n) = \bar{x}(n-1) - \bar{x}(n) \quad (9)$$

This study applies the scheme to the one-dimensional signal, we get the following relation**:** (Piella and Pesquet-Popescu 2007).

$$\bar{x}(n) = \begin{cases} \dfrac{x(n)+y(n)}{2} & \text{if } |y(n)-x(n)| \prec T \\ x(n) & \text{otherwise} \end{cases} \quad (10)$$

$$\bar{Y}(n) = \begin{cases} y(n)-x(n) & \text{if } |\bar{x}(n-1)-\bar{x}(n)| \prec \bar{T} \\ \dfrac{y(n)-x(n)}{1+|\bar{x}(n-1)-\bar{x}(n)|} & \text{otherwise} \end{cases} \quad (11)$$

## 4. Experimental testing

**4.1. Test Bench Details**

In our case, the experimental testing is given in figure 5 where the induction machine is used to test the performance of the proposed methodology identifying the fault treated in this work.

The tested induction motor characteristics are presented in table1.

The electrical scheme consists of a series of universal symbols that accurately describe the installation; this presentation of the circuit of experiment is shown in figure 6.

The main idea of this study is to be able to simulate electrical faults in an asynchronous machine (with a variety of failures) in order to obtain oscillograms (variables that can be measured) on which ones that can be analyzed spectral signatures of these defects. The machine is tested under 2 steps of load: at no load case and at full load case we compare between the spectra of the current in healthy and faulty conditions.

**Table 1.** Induction motor characteristics.

| | |
|---|---|
| Rated frequency | 50Hz |
| Number of pole pairs | 2 |
| Number of rotor bars | 28 |
| Rated Voltage | 380V |
| Rated Power | 3kw |

**Fig.5.** Experimental setup for outer race defect

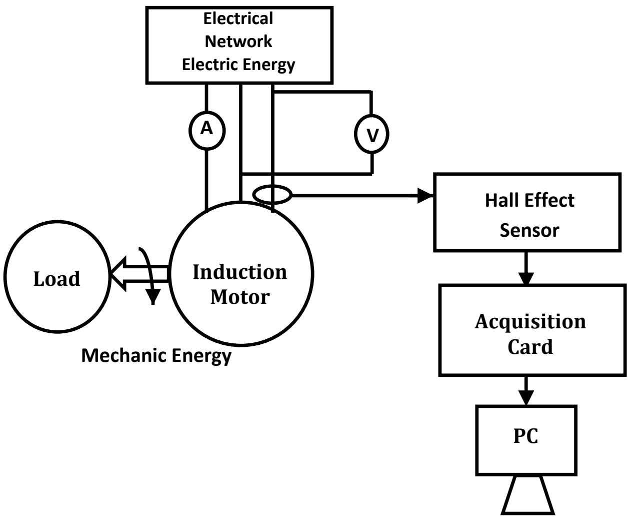


**Fig.6.** Electrical scheme of the circuit of experiment.

### 4.2. Outer race defect

The equation that calculates the characteristic frequencies of the bearing elements fault presented in (Bouzida et al. 2017):

$$f_{bearing\ defect} = \left| f_{su} \pm {}_{k} f_{c} \right| \quad (12)$$

With: k=1, 2, 3...; $f_{su}$ the supply frequency; $f_c$ one of the characteristic frequencies.

For bearings balls between 6 and 12, the characteristic frequencies for outer race fault presented by:

$$f_c = f_0 = 0.4 N_b f_r \quad \text{for outer race fault}$$

$$f_{or_k}^{\pm} = \left| f_{su} \pm k.0.4\, N_b.f_r \right| \quad (13)$$

#### 4.2.1. at no load case

**Lifting method**

Figures (7), (8) respectively show the details of d1 to d5 from the lifting method in healthy (blue) and faulty (red), (purple) machine under no load case. Our results have a part of the analysis, variability of the stator current for different levels with many tests under the same conditions this analysis presented the variation of some signals.

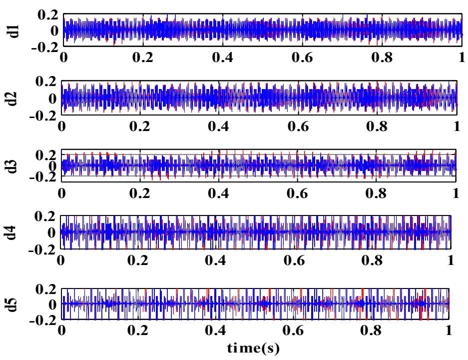


**Fig.7.** First test of experimental stator current details from the lifting method in healthy and faulty machine at no load with outer raceway defect (s=0).

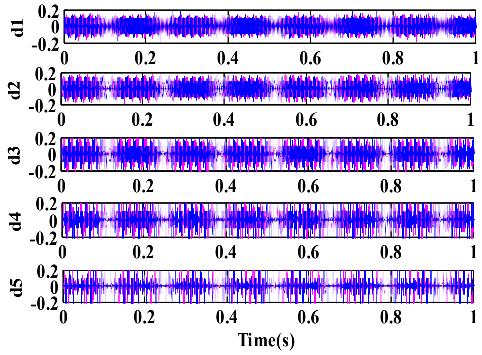


**Fig.8.** Second test of experimental stator current details of the lifting method in healthy and faulty machine at no load with outer raceway defect (s=0).

The frequency spectra of stator current are obtained thanks to the lifting method.

Figure 9 presented the characteristic frequencies correspondent the detail d2 of the stator current spectrum of healthy (blue) and faulty (red) asynchronous motor under no load condition by lifting method.

The characteristic frequencies correspondent the detail d2 of the stator current spectrum of healthy (blue) and faulty (purple) asynchronous motor under no load condition by lifting method are indicated in figure 10.

The characteristic faults frequencies clearly appear on the stator current spectrum in comparison to the healthy case. This validates the proposed theoretical approach which assumes the variations at the characteristic frequency as a consequence of the bearing fault. We observe that the characteristic frequencies of the faults obtained have acceptable amplitude.

Another series of harmonics appear in the spectrum of detail number 2 in first test at e.g. 37.1 Hz, 44.3 Hz, 55.7Hz, 144.2Hz, and 148.5Hz.In second test we have noticed another series of harmonics in the spectrum of detail number 2 such as: 44.2 Hz, 55.7Hz, 144.1Hz, and 148.5Hz. For a better overview, the characteristic frequencies and the amplitudes of outer race defect signatures are illustrated in Table 2.

**According to the FFT of the current:**

As an illustration first test and the second test of the stator current spectrum of healthy and faulty motor at no load condition by the FFT technique are shown in figure 11 and figure 12 respectively.

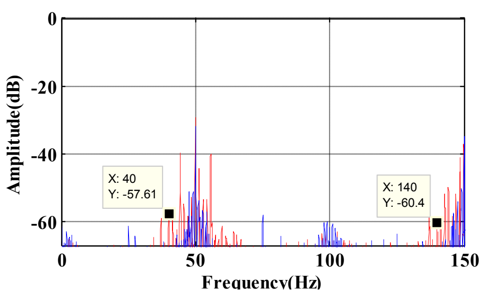


**Fig.9 .** First test of d2 of stator current spectrum of healthy and faulty motor at no load by the lifting method with outer raceway defect (s=0).

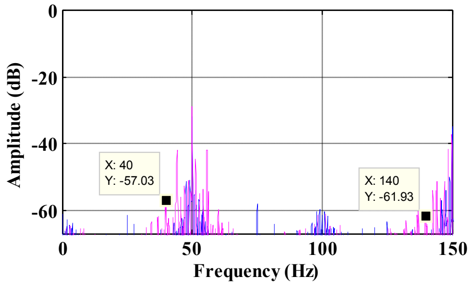


**Fig.10** . Second test of d2 of stator current spectrum of healthy and faulty motor at no load by the lifting with outer raceway defect (s=0).

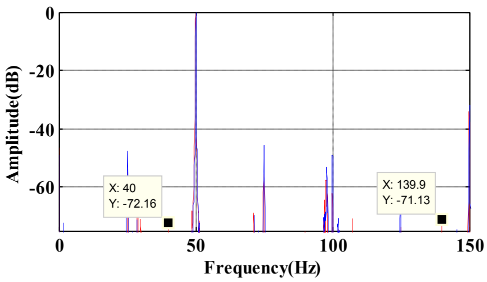


**Fig.11 .** First test of stator current spectrum of healthy (blue) and faulty (red) motor at no load by FFT technique with outer raceway defect (s=0).

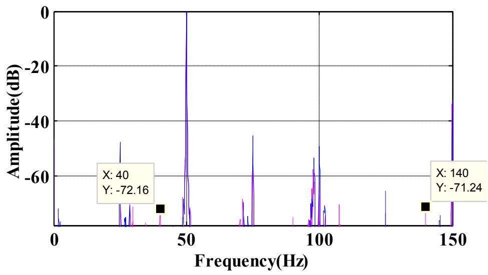


**Fig.12.** Second test of stator current spectrum of healthy (blue) and faulty (purple) motor at no load by FFT technique with outer raceway defect (s=0).

**Table 2.** Characteristic frequencies of outer race defect at no load by lifting method.

| | | | |
|---|---|---|---|
| Formula of characteristic frequencies | | (a) | (b) |
| Theoretical values (Hz) | | 40 | 140 |
| First test | Experimental Values (Hz) | 40 | 140 |
| | Amplitudes (dB) | -57.61 | -60.4 |
| Second test | Experimental Values(Hz) | 40 | 140 |
| | Amplitudes (dB) | -57.03 | -61.93 |

$(a): f_{or1}^{-} = |f_{su} - f_c| = |f_{su} - 0.4N_b f_r|;\ (b): f_{or1}^{+} = |f_{su} + f_c| = |f_{su} + 0.4N_b f_r|$

Tables 3 illustrate the characteristic frequencies and the amplitudes of outer race defect. The results obtained by this method are confounded with the formula of characteristic frequencies of the defect; without forgetting to take in consideration the phenomena to the tests that influence for example to the slip also. We can notice precisely the absence of additional harmonics in stator current spectrum comparing the lifting method. Comparing the results shown in Table 2 and Table 3 we find an excellent concordance and a complete agreement between the theoretical and experimental values of characteristic frequencies with amplitudes acceptable. We notice that the results in both techniques are very clear and acceptable. The characteristic frequencies are so clear in comparison with the healthy state.

**Table 3.The** characteristic frequencies of outer race defect at no load by FFT technique.

| | | | |
|---|---|---|---|
| Formula of characteristic frequencies | | (a) | (b) |
| Theoretical values (Hz) | | 40 | 140 |
| First test | Experimental Values (Hz) | 40 | 139.9 |
| | Amplitudes (dB) | -72.16 | -71.13 |
| Second test | Experimental Values(Hz) | 40 | 140 |
| | Amplitudes (dB) | 72.16.03 | -71.24 |

$(a): f_{or1}^{-} = |f_{su} - f_c| = |f_{su} - 0.4N_b f_r|;\ (b): f_{or1}^{+} = |f_{su} + f_c| = |f_{su} + 0.4N_b f_r|$

### 4.2. 2. At full load case

**Lifting method**

The frequency spectra of stator current are obtained thanks to the lifting method.

As an illustration, figure 13 shows the characteristic frequencies corresponding to the detail d2 of the stator current spectrum of healthy (blue) and faulty (red) motor at full load condition by lifting method.

The characteristic frequencies correspondent the detail d2 of the stator current spectrum of healthy (blue) and faulty (purple) asynchronous motor under full load condition by lifting method are presented in figure 14.

We clearly notice the presence of harmonics related to the outer race defect. If we pay attention to the spectrum of detail 2 in the defective state such as: 17 Hz, 82.9 Hz, 117Hz in first test and 17 Hz, 82.9 Hz, 117.1Hz … for second test.

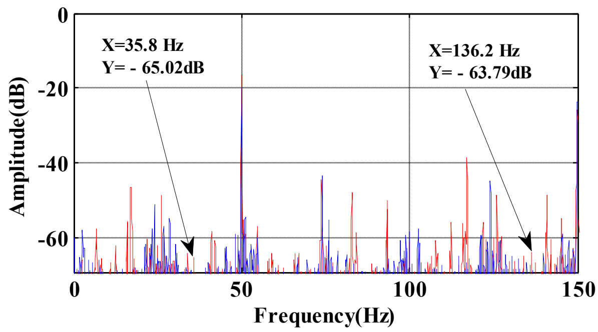


**Fig.13.** First test of d2 of stator current spectrum of healthy and faulty motor at full load by the lifting method with outer raceway defect (s=0.044).

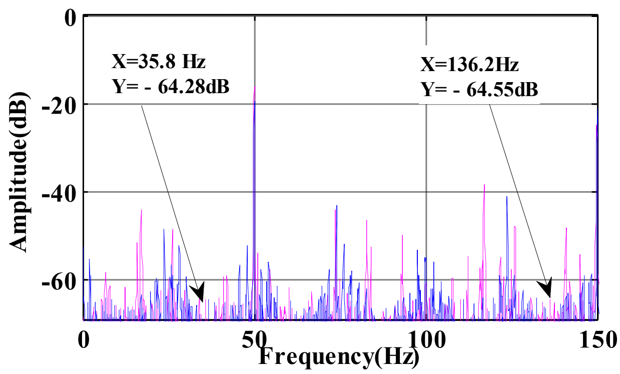


**Fig.14.** Second test of d2 of stator current spectrum of healthy and faulty motor at full load by the lifting method with outer raceway defect (s=0.044).

Table 4 represents some comparison values between the theory and the experimental characteristic frequencies of outer race defect signatures.

In the both experiments we recorded almost the same results and this shows that this method is determined and localized well the outer race fault.

This successful comparison of the experimental results with the characteristic frequency formulas of the outer race defect allows ensuring the effectiveness of the diagnostic method by the application based on an adaptive wavelet transform which is constructed with a three-step nonlinear lifting scheme especially at the amplitudes level , we notice that the analysis of the healthy experimental spectra shows the absence of the characteristic frequencies fault in the spectrum of the d2 of stator current .

**FFT technique**

To well distinguish between the healthy and faulty conditions figure 15 and 16 respectively show the characteristic frequencies correspondent the stator current spectrum of healthy (blue) and faulty (red),(purple) motor of the asynchronous motor at full load by FFT technique with outer raceway defect.

The characteristic frequencies are so clear in comparison with the healthy state so the results are very clear and acceptable.

The characteristic frequencies correspondent the outer race defect under FFT technique is presented in table 5.

The comparison between the theoretical and experimental results shown in Table 4 and Table 5 present a good concordance and a complete agreement between the values of characteristic frequencies with amplitudes acceptable.

The diagnostic operation of the current by this method will allow an acceptable follow-up of the outer race defect indicators.

Our study noted the absence of additional frequencies. The experimental results obtained confirm the accuracy and validation of the theoretical results.

**Table.4**. Characteristic frequencies of outer race defect at full load by the lifting method.

| Formula of characteristic frequencies | | (a) | (b) |
|---|---|---|---|
| Theoretical values (Hz) | | 36.04 | 136.04 |
| First test | Experimental Values (Hz) | 35.8 | 136.2 |
| | Amplitudes (dB) | -65.02 | -63.79 |
| Second test | Experimental Values(Hz) | 35.8 | 136.2 |
| | Amplitudes (dB) | -64.28 | -64.55 |

$(a): f_{or1}^{-} = |f_{su} - f_c| = |f_{su} - 0.4 N_b f_r|$; $(b): f_{or1}^{+} = |f_{su} + f_c| = |f_{su} + 0.4 N_b f_r|$

**Table.5**. Characteristic frequencies of outer race defect at full load by the lifting method.

| Formula of characteristic frequencies | | (a) | (b) |
|---|---|---|---|
| Theoretical values (Hz) | | 36.04 | 136.04 |
| First test | Experimental Values (Hz) | 36 | 136 |
| | Amplitudes (dB) | -75.02 | -72.52 |
| Second test | Experimental Values(Hz) | 36 | 136 |
| | Amplitudes (dB) | -76.42 | -73.67 |

$(a): f_{or1}^{-} = |f_{su} - f_c| = |f_{su} - 0.4 N_b f_r|$; $(b): f_{or1}^{+} = |f_{su} + f_c| = |f_{su} + 0.4 N_b f_r|$

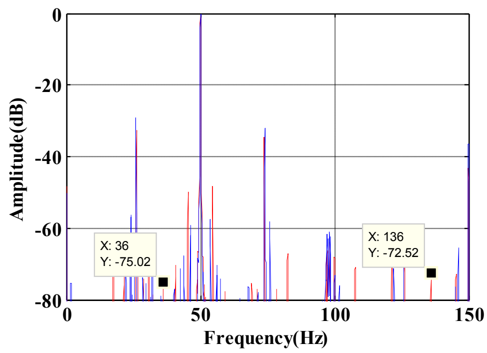


**Fig.15.** first test of stator current spectrum of healthy (blue) and faulty (red) motor at full load by FFT technique with outer raceway defect (s=0.044).

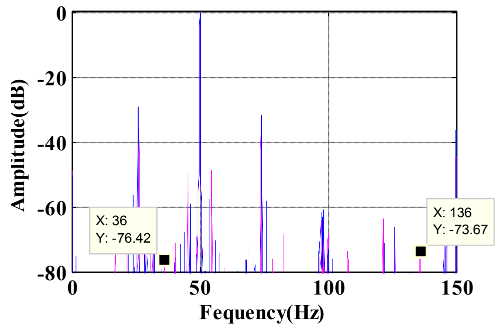


**Fig.16**. Second test of stator current spectrum of healthy (blue) and faulty (purple) motor at full load by FFT technique with outer raceway defect (s=0.044).

Moreover, Depending on the spectrum of the stator current and the theatrical equation we will give some examples of the characteristic frequencies.

$$f_{or_k}^{\pm} = |f_{su} \pm k\,.0.4\,N_b\,.f_r|$$

With $f_{su}$ =50 Hz, $N_b$ =9, $f_r = \frac{1-S}{P}.f_{su}$ ($S$=0.044) and $P$=2,

$$f_r = \frac{1-0.044}{2}.50 = 23.9\ Hz$$

$$f_{or^-} = 50 - (0.4).9\,.\,23.9$$

$$f_{or^-} = 36.04\ Hz$$

$$f_{or^+} = f_s + 0.4 N_b\,.f_r$$

$$f_{or+} = 136.04\ Hz$$

The comparison between the theoretical and experimental results shown in Table 4 and Table 5 present a good concordance and a complete agreement between the values of characteristic frequencies with amplitudes acceptable.

We have compared our method with the discrete wavelet transforms (DWT) under the same conditions and the same induction motor characteristics (Bessous et al. 2016a).

Another detection method must be used similar to time–frequency analysis or discrete wavelet transforms (DWT), the comparison between the results obtained by this method and the adaptive wavelet transform which is based on a three-step nonlinear lifting scheme: a fixed prediction followed by a space-varying update and a no additive prediction for the detection of bearing faults on induction motor stator current are confounded with the formula of characteristic frequencies of the defect; without forgetting to take in consideration the phenomena to the tests that influence for example to the slip also. Indicating that (Bessous and al. 2016b) showed that the detail 6 is rich in fault signal information but in our method the detail 2 is rich in fault signal information.

## Conclusion

The important information in the signals can be exploited flexibly by a novel application adaptive wavelet transform method. This work presents a new method based on the application of the three-step nonlinear lifting scheme for the diagnosis of outer raceway defects which is one of the current topics for many researchers and we have been interested in the analysis of the characteristic frequency components in the detail signals of the stator current spectrum under different conditions (no-load and full load) with many experiments.

The comparisons of the results between the two techniques confirm the effectiveness of the last one (the three -step nonlinear lifting**)** with a good amplitude values. The adaptive lifting method ensures that the results obtained by the application of the three-step nonlinear lifting scheme are confounded with the formula of characteristic frequencies of the defect; without forgetting to take in consideration the phenomena to the tests that influence for example to the slip also .Otherwise, the details are rich with supplementary harmonics that have important amplitude. We will implement the method proposed in non stationary signals using different faults and under different conditions.

## References

Barman, D., S. Sarkar, G. Das, S. Dasa & P. Purkait (2015) DFA and DWT based severity detection and discrimination of induction motor stator winding short circuit fault from incipient insulation failure. Electrical, Electronics, Signals, Communication and Optimization (EESCO), International Conference, IEEE, pp. 1-6.

Bessous, N., S.E. Zouzou , W. Bentrah & S. Sbaa (2015) A comparative study between the FFT and DWT method applied to a bearing fault in induction motors. Wseas transactions on systems and control.

Bessous, N., S.E. Zouzou , W. Bentrah & S. Sbaa (2016a) Detection and diagnosis of static eccentricity fault in induction machines using the MCSA and DWT method. International Conference on Electrical Sciences and Technologies, CISTEM, Marrakesh, Morocco.

Bessous, N., S.E. Zouzou, W. Bentrah, S. Sbaa, M. Sahraoui (2016b) Diagnosis of bearing defects in induction motors using discrete wavelet transform. International Journal of System Assurance Engineering and Management 9(2) 335-343.

Blödt, M., P. Granjon, B. Raison, G. Rostaing (2004) Models for bearings damage detection in induction motors using stator current monitoring. International Symposium on Industrial Electronics, IEEE Vol. 1: 383-388.

Bonnett, A.H., G.C. Soukup (1992) Cause and analysis of stator and rotor failures in three-phase squirrel-cage induction motors. Industry Applications, IEEE Transactions on Industry Applications 28(4): 921-937.

Bouzida, A., R. Abdelli, O. Touhami (2017) Experimental analysis of dynamic eccentricity in induction machine using motor current signature analysis and discrete wavelet transform. Revue Romaine des Sciences Techniques - Serie Électrotechnique et Énergétique 62(2): 142-147.

Gyftakis, K., N.J.C. Kappatou (2013) A novel and effective method of static eccentricity diagnosis in three-phase induction motors. IEEE Transactions on Energy Conversion 28: 405-412.

Heijmans, H.J.A.M., B. Pesquet-Popescu, G. Piella (2005) Building non redundant adaptive wavelets by update lifting. Applied and Computational Harmonic Analysis 18: 252-281.

Heijmans, H.J.A.M., G. Piella, B. Pesquet-Popescu, G. Pau (2006) Combining semi norms in adaptive lifting schemes and applications to image analysis and compression. Journal of Mathematical Imaging and Vision 25: 203-226.

Karvelis, P., G. Georgoulas, I.P. Tsoumas, J.A. Antonino-Daviu, V.Climente-Alarcon, C.D. Stylios (2015) A Symbolic representation approach for the Diagnosis of broken rotor bars in induction motors. IEEE Trans. Industrial Informatics 11(5): 1028-1037.

Lebaroud, A., C. Guy (2011) Study of Rotor Asymmetry Effects of an Induction Machine by Finite Element Method. Journal of Electrical Engineering and Technology 6: 342-349.

Mabrouk, A.E., S.E. Zouzou, S. Khelif (2017) On-line fault diagnostics in operating three phase induction motors by the active and reactive currents. International Journal of System Assurance Engineering and Management 8(1): 160-168.

Oumaamar, M.E.K.F. Babaa, A. Khezzar, M. Boucherma, F. Meıbody-Tabar (2005) Novel method of broken rotor bars diagnosis in induction machine by D.C supply. 6th international symposium on advanced electro mechanical motion systems electro motion, Lausanne.

Piella, G., B. Pesquet-Popescu (2007) A three-step nonlinear lifting scheme for lossless image compression. International Conference on Image Processing, ICIP 2007, IEEE, Vol. 1, pp. 453-456.

Piella, G., G. Pau, B. Pesquet-Popescu (2005) Adaptive lifting schemes combining seminorms for lossless image compression. IEEE International Conference on Image Processing, ICIP 2005, IEEE, Vol. 1, p. 753.

Saidi, L. (2017) The deterministic bispectrum of coupled harmonic random signals and its application to rotor faults diagnosis considering noise immunity. Applied Acoustics 122: 72-87.

Wang, D., Y. Zhao, C. Yi, K. l. Tsui & J. Lin (2018) Sparsity guided empirical wavelet transform for fault diagnosis of rolling element bearings. Mechanical Systems and Signal Processing 101: 292-308.

Yahia, K., A.J.M. Cardoso, A. Ghoggal, S.E. Zouzou (2014) Induction motors air-gap-eccentricity detection through the discrete wavelet transform of the apparent power signal under non-stationary operating conditions. ISA transactions 53(2): 603-611.

Yang, C., T.J. Kang, D. Hyun, S.B. Lee, J.A. Antonino-Daviu, J. Pons-Llinares (2014) Reliable Detection of Induction Motor Rotor Faults Under the Rotor Axial Air Duct Influence. IEEE Transactions on Industry Applications 50(4): 2508-2515.